Journal of Power Sources 189 (2009) 982–987

Contents lists available at ScienceDirect

Journal of Power Sources

journal homepage: www.elsevier.com/locate/jpowsour

Synthesis of Pd/TiO_2 nanotubes/Ti for oxygen reduction reaction in acidic solution

Y. Fu [a], Z.D. Wei [a,b,*], S.G. Chen [b], L. Li [b], Y.C. Feng [a], Y.Q. Wang [b], X.L. Ma [a], M.J. Liao [a], P.K. Shen [c,**], S.P. Jiang [d]

[a] State Key Laboratory of Power Transmission Equipment & System Security and New Technology, School of Chemistry and Chemical Engineering, Chongqing University, Chongqing 400044, China
[b] School of Material Science and Engineering, Chongqing University, Chongqing 400044, China
[c] The State Key Laboratory of Optoelectronic Materials and Technologies, School of Physics and Engineering, Sun Yat-Sen University, Guangzhou 510275, China
[d] School of Mechanical and Aerospace Engineering, Nanyang Technological University, 50 Nanyang Avenue, Singapore 639798, Singapore

ARTICLE INFO

Article history:
Received 12 December 2008
Accepted 15 December 2008
Available online 25 December 2008

Keywords:
Oxygen reduction reaction
Electrocatalysis
TiO_2 nanotubes
Pd
Fuel cells

ABSTRACT

Highly ordered and uniformly distributed TiO_2 nanotubes on a pure titanium substrate (TNTs/Ti) are successfully fabricated by a pulse anodic oxidation method as the support for Pd electrocatalyst. Pd is electrochemically deposited onto TNTs/Ti support. The sensitization with $SnCl_2$ and activation with $PdCl_2$ are critical for the formation of highly dispersed Pd nanoparticles on the TNTs/Ti support. It has been found that both Pd/TNTs/Ti and Pt electrodes show the similar electrochemical behavior in H_2SO_4, implying the possibility to develop the Pt-free alternative electrocatalyst based on the Pd/TNTs/Ti system in acid medium. The preliminary results in this work show that the Pd/TNTs/Ti catalysts have an acceptable catalytic activity for the oxygen reduction reaction (ORR) in acid medium. The factors influencing the structure of TNTs and the catalytic activity of Pd/TNTs/Ti for the ORR are also studied in detail.

1. Introduction

For decades, Pt and Pt-based alloys have been widely used as the electrocatalysts for the oxygen reduction reaction (ORR) in proton exchange membrane and direct methanol fuel cells (PEMFCs and DMFCs). However, it is well-known that platinum is a precious metal and is scarcely available. The high price and limited resources of platinum hinder the commercial viability of PEMFCs and DMFCs. Thus, the development of the Pt-free alternative electrocatalysts is important for the technological development of fuel cells. There have been significant studies on the transition metal-based catalysts as the Pt-free alternative electrocatalysts [1–4]. On the other hand, palladium is an interesting alternative catalyst as palladium is not only significantly cheaper than platinum but also at least fifty times more abundant in the earth as compared to Pt. Pd-based catalysts have been studied for the ORR and methanol electro-oxidation reactions for the low temperature fuel cells and exhibit a considerable catalytic activity [5–8]. In particular, Pd-based electrocatalysts have an excellent tolerance to methanol poisoning [9].

In order to improve the utilization efficiency of the noble metal catalysts, the noble metal nanoparticles are usually dispersed on an inert high area support. The most widely used catalyst support is the high surface area amorphous carbon. However, carbon as the electrocatalyst support could be corroded chemically and/or electrochemically under the fuel cell operation environment which could lead to the detachment and loss of the noble metal nanoparticles and thus the electrochemical activity [10]. In searching for novel and stable support for the noble metal catalysts, TiO_2 nanotubes (TNTs) come into sight because of their good physical and chemical properties and high stability in acidic and alkaline solutions. In addition, our recent quantum chemistry study indicates that TiO_2 can improve the HOMO orbital spatial size of Pd and weaken the adsorption of atomic oxygen on Pd in comparison with Pd supported on carbon [11]. TNTs can be synthesized by different methods including sol–gel [12], hydrothermal [13], template [14] and anodic oxidation [15–18]. The applications of TNTs in dye-sensitized solar cell, photo-catalysts and heterogeneous catalysts have also been reported [18–21].

Obviously, if TNTs can be directly produced on a metallic Ti substrate by the anodic oxidation method, it would be advantageous and convenient for fuel cell applications where an electric current collector is required. Moreover, the morphology and the structure of the TNT layer can also be easily modulated by changing the anodic oxidation conditions.

Fig. 1 shows the cyclic voltammograms (CV) of Pt/C, Pd/TNTs/Ti and Pt sheet in 0.5 M H_2SO_4. It can be seen that all the electrodes

* Corresponding author at: School of Chemistry and Chemical Engineering, Chongqing University, Chongqing 400044, China. Tel.: +86 23 60891548; fax: +86 23 65106253.
** Corresponding author.
E-mail addresses: zdwei@cqu.edu.cn (Z.D. Wei), stsspk@sysu.edu.cn (P.K. Shen).

0378-7753/$ – see front matter © 2008 Elsevier B.V. All rights reserved.
doi:10.1016/j.jpowsour.2008.12.065

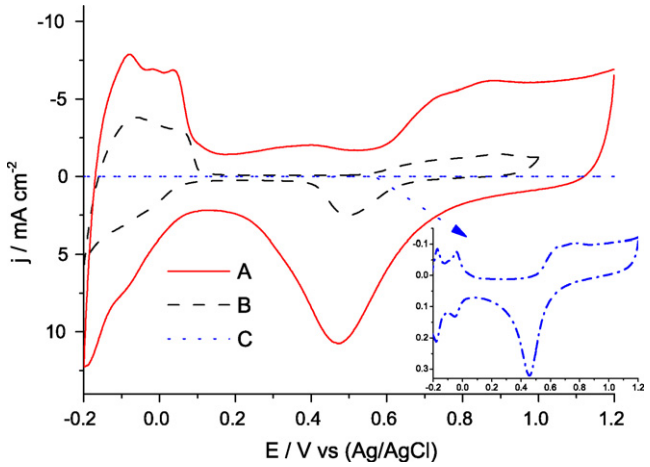

Fig. 1. CVs (A) of Pt/C, (B) Pd/TNTs/Ti and (C) Pt sheet in 0.5 M H_2SO_4. The metal catalyst loadings were 0.27 mg cm^{-2} for Pt/C and 0.32 mg cm^{-2} for Pd/TNTs/Ti.

show a similar CV behavior. This indicates that it is feasible to use Pd/TNTs/Ti as the Pt-free alternative catalyst for methanol oxidation, hydrogen oxidation, oxygen reduction, hydrogenation of nitrobenzene and so on. Here, we report the preparation and application of Pd/TNTs/Ti for the oxygen reduction reaction (ORR) in fuel cells. The influence of the preparation conditions on the performance of the Pd/TNTs/Ti electrode is studied in detail.

2. Experimental

2.1. Preparation of TNTs/Ti catalyst support

Ordered TNT arrays were produced on a pure Ti sheet (10 mm × 50 mm × 1 mm, 99.7% purity) by an asymmetric pulse anodic oxidation method in a 1 M H_2SO_4 + 0.5 wt% HF electrolyte solution. The Ti sheet was mechanically and chemically polished to a high mirror finish in a mixture of HF:HNO_3:H_2O with 1:3:5 in volume, followed by rinsing thoroughly with DI water. The unexposed part of the electrodes was shielded with epoxy resin, leaving an area of 1 cm^2 open to the electrolyte solution. A two-electrode electrochemical cell consisting of the Ti sheet anode and a piece of 5 cm × 5 cm carbon paper cathode were used for the anodic oxidation of Ti sheet. An anodic pulse oxidation was performed at an average oxidation current density of 0.5 A cm^{-2} for 0.9 ms current-on and 0.1 ms current-off, followed by a cathodic pulse reduction at an average reduction current density of 0.04 A cm^{-2} for 0.6 ms current-on and 0.4 ms current-off after each anodic pulse for 20 min. The cathodic reduction pulse was used to remove the heat and stir the electrolyte by means of generating a large amount of hydrogen bubbles. TNTs/Ti was then ultrasonically cleaned in a mixture of acetone, isopropyl alcohol and ethanol, rinsed with DI water and dried in a vacuum oven. To increase the crystallinity, TNTs/Ti was annealed in air at 480 °C in a muffle furnace for 3 h and then cooled to room temperature at 5 °C min^{-1}. TNTs/Ti prepared by a direct current oxidation method according to a previous report [15] was used for comparison.

2.2. Preparation of Pd/TNTs/Ti electrodes

Pd/TNTs/Ti electrodes were prepared by the electrodeposition of Pd on as-prepared TNTs/Ti support. Electrodeposition experiments were carried out at a water-bath thermostat. Prior to the electrodeposition of Pd, the substrate TNTs/Ti was first sensitized in 0.5 g $SnCl_2$ + 0.56 M HCl for 5 min, and then activated in 0.05 M $PdCl_2$ + 0.5 M HCl for 1 min. Pd^{2+} ions were reduced to metallic Pd by the adsorbed Sn^{2+} ions on the surface of TNTs/Ti. The Pd particles reduced by Sn^{2+} ions would serve as the crystalline seeds for the succeeding Pd electrodeposition. Pd electrodeposition was conducted for 15 s at a pulse peak current of 100 mA cm^{-2} with 300 μs current-on and 700 μs current-off.

2.3. Morphology characterization

The XRD analysis of the TNTs/Ti substrate was carried out on a diffractometer (D/max-1200, Japan) using a Cu Kα X-ray source operating at 45 kV and 100 mA, scanning at the rate of 4° min^{-1} with a 2θ angular resolution of 0.05°. The morphologies of the TNTs/Ti and Pd/TNTs/Ti were measured using a FEI Nova 400 field emission scanning electron microscope (FESEM) from Netherlands (Peabody, MA). Cross-section of TNTs/Ti samples was examined by SEM.

2.4. Electrochemical measurement

Electrochemical experiments were performed on a CHI 660B electrochemical workstation (Chenhua, China) in a standard three-electrode cell. The platinum wire was employed as the counter electrode. Electrode potential in this paper was referred to a saturated Ag/AgCl reference electrode. All experiments were carried out at room temperature (24 ± 2 °C).

3. Results and discussion

3.1. Influence of current pattern in anodic oxidation

Fig. 2 shows the scanning electron micrographs of a TNTs/Ti substrate prepared by the pulse anodic oxidation (Fig. 2a$_1$ and a$_2$) and direct current oxidation (Fig. 2a$_3$) methods. Fig. 2a$_2$ and a$_3$ are the images of TNTs/Ti after annealed in air at 480 °C. It shows

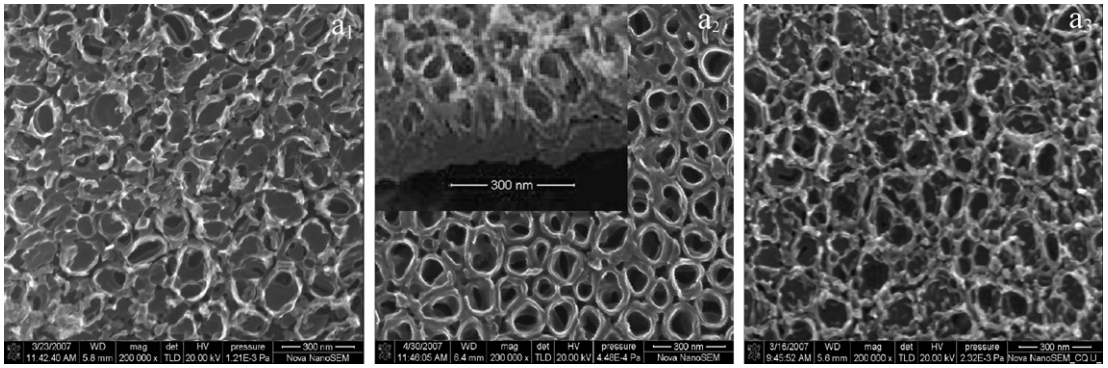

Fig. 2. FESEM micrographs of (a$_1$) TNTs/Ti prepared by pulse anodic oxidation, (a$_2$) after annealed at 480 °C and (a$_3$) TiO_2/Ti prepared by direct current oxidation and annealed at 480 °C. The inset in a$_2$ is the FESEM of the cross-sectional view of sample a$_2$.

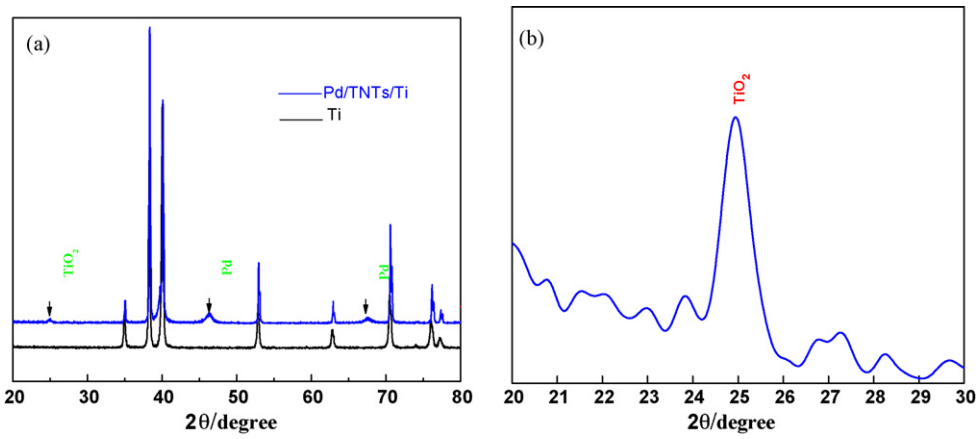

Fig. 3. XRD patterns of Pd/TNTs/Ti and Ti substrate.

that the highly ordered and uniform TNTs can only be obtained by the pulse current anodic oxidation method after annealing at 480 °C. The TNTs with 80 nm in diameter, 20 nm in wall thickness and ~300 nm in length are shown in the inset of Fig. 2a$_2$. Evidently, the annealing step is indispensable for the freshly yielded TiO_2 as shown in Fig. 2a$_1$ to form a highly ordered and uniform crystalline TiO_2. Although a highly ordered and uniform crystalline TiO_2 was successfully fabricated by the direct anodic current oxidation method as described in the previous report [18], we could not be able to reproduce in the present work. The possible reason could be due to the difference in the experimental temperature. The influence of the electrolyte temperature on the TNTs formation in the case of the pulse anodic current oxidation method may not be as serious as in the case of the direct anodic current oxidation method because the anodic oxidation only lasts for 20 min in the case of pulse anodic current oxidation and it requires 3 h in the case of direct anodic current oxidation. Thus, the heat accumulation in the case of pulse anodic current oxidation process is not as serious as that in the case of direct anodic current oxidation process. In addition, a cathodic reduction pulse associated with the pulse anodic oxidation method will remove the accumulated heat and stir the electrolyte by the generation of a large amount of hydrogen bubbles. Generally, the low temperature is beneficial for the formation of highly ordered nanostructures. It is apparent that the pulse anodic oxidation is superior to the direct anodic current oxidation for the production of highly ordered and uniform crystalline TiO_2 nanotubes in terms of time-saving and maintenance of low operational temperatures.

Fig. 3a shows the XRD patterns of Pd/TNTs/Ti in which the substrate TNTs/Ti was annealed in air at 480 °C for 3 h. The microstructure of TNTs/Ti substrate can be seen in Fig. 2a$_2$. A weak diffraction peak in Fig. 3a at the 2θ of 25° confirms the presence of anatase TiO_2. The weak diffraction peak of anatase TiO_2 is magnified and displayed in Fig. 3b. The diffraction peaks at the 2θ of 46.49° and 68.08° correspond to (2 0 0) and (2 2 0) facets of the Pd crystal.

Fig. 4 presents the cyclic voltammograms (CVs) of Pd/TNTs/Ti in an N_2 saturated 0.5 M H_2SO_4 solution at scan rate of 50 mV s^{-1} (Fig. 4a) and the linear scan curves (LSV) of Pd/TNTs/Ti for ORR in an O_2 saturated 0.5 M H_2SO_4 solution at scan rate of 1 mV s^{-1} (Fig. 4b). Pd was electrodeposited on TNTs/Ti substrate by a pulse current for 15 s at a pulse peak current of 100 mA cm^{-2} for 300 μs current-on and 700 μs current-off. The a$_2$ and a$_3$ in Fig. 4 denote that TNTs/Ti supports were prepared by the pulse anodic current oxidation method and by the direct anodic current oxidation method, respectively. Apparently, the catalytic activity of Pd supported on TNTs/Ti by the pulse anodic current oxidation is superior to that by the direct anodic current oxidation.

3.2. Influence of HF concentration on morphology of produced TiO_2

Chemical dissolution of TiO_2 in the HF-containing electrolyte plays a key role in selectively forming nanotubes rather than simple nanoparticle structures. Fig. 5 shows the SEM images of an annealed TiO_2 prepared in 1 M H_2SO_4 with different concentrations of HF by

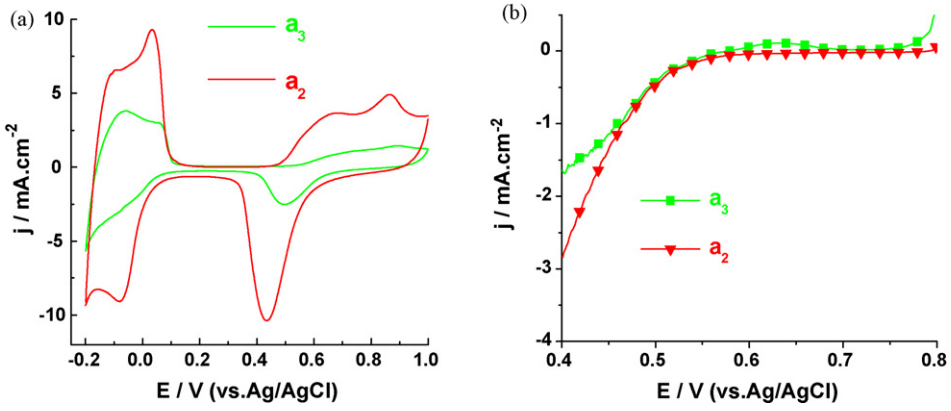

Fig. 4. CVs of Pd/TNTs/Ti in N_2 saturated 0.5 M H_2SO_4 solution at scan rate of 50 mV s^{-1} (a) and LSV of Pd/TNTs/Ti for ORR in O_2 saturated 0.5 M H_2SO_4 solution at scan rate of 1 mV s^{-1} (b). (a$_2$ and a$_3$ denote that the substrates TNTs/Ti were prepared by pulse anodic current oxidation as shown in Fig. 2a$_2$ and by direct anodic current oxidation in Fig. 2a$_3$, respectively.)

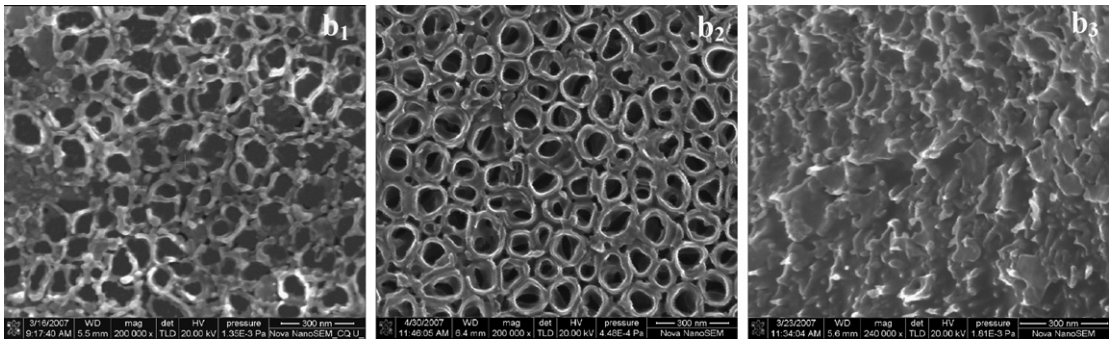

Fig. 5. SEM images of TiO_2 films prepared at different concentration of HF: (b_1) 0.1 wt%, (b_2) 0.5 wt% HF, (b_3) 2 wt% HF.

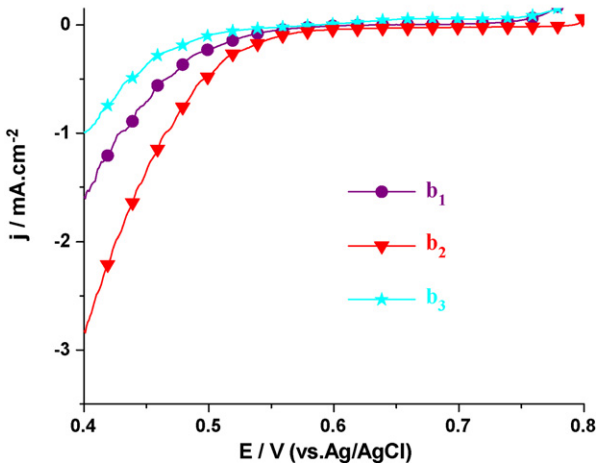

Fig. 6. LSV curves of ORR on Pd/TNTs/Ti at 1 mV s^{-1} where b_1, b_2 and b_3 denote the substrates TNTs/Ti as described in Fig. 5.

the pulse anodic current oxidation method for 20 min. A lower concentration of HF means a lower chemical etching rate and a higher concentration of HF means a higher chemical etching rate. There is a balance between the TiO_2 electrochemical formation and the TiO_2 chemical dissolution for obtaining a highly ordered and uniform crystalline TiO_2. Thus, the TNTs could not be properly formed both at too low or too high HF concentrations as shown in Fig. 5b_1 and b_3.

Fig. 6 presents the LSVs for ORR on the Pd catalysts prepared on a TNTs/Ti support as described in Fig. 5. The highest current of ORR was obtained on the TNTs/Ti support with the morphology as shown in Fig. 5b_2. Once again, it confirms that the uniform and highly ordered TNTs arrays with open structure are critical for the high electrochemical activity of Pd/TNTs/Ti catalysts.

3.3. Influence of anodic oxidation time

To understand the process of nanotubes formation, TiO_2 was synthesized at different pulse anodic current oxidation time. The SEM images of the prepared TiO_2 after annealed in air at 480 °C are shown in Fig. 7. The TiO_2 nanotube formation begins with small pits that will act as pore forming centers as shown in Fig. 7c_1. With the proceeding of the pulse anodic current oxidation, the top surface of a fully developed nanotubes array starts to form (Fig. 7c_2). When the pulse anodic current oxidation continues for 50 min, cracks appear on the TNTs array as can be seen in Fig. 7c_3. The reason could be that longer anodic oxidation time forms longer TiO_2 nanotubes that could not sustain the balance between the TiO_2 electrochemical formation and the TiO_2 chemical dissolution. Fig. 8 shows the LSVs of the ORR on the Pd deposited on the TNTs/Ti support as described in Fig. 7. The results are consistent with the foregoing discussion.

3.4. Influence of sensitization and activation

Fig. 9 shows the SEM images of Pd deposited on the TNTs/Ti supports treated at different sensitization and activation conditions. The results indicate that it is very important to control the conditions of sensitization and activation on the surface of TNTs/Ti before the Pd electrodeposition in order to obtain the highly dispersed Pd deposits. The highly dispersed Pd deposits can only be obtained on the TNTs/Ti support that has been loaded in advance a proper amount of highly dispersed active Pd seeds through the sensitization in 0.5 g $SnCl_2$ dissolved in 0.56 M HCl for 5 min and then the activation in 0.05 M $PdCl_2$ dissolved in 0.5 M HCl for 1 min. The proper amounts of highly dispersed active Pd seeds would significantly affect the dispersion of final Pd deposits via electrodeposition. Such a proper amount of highly dispersed active Pd seeds can be obtained through a proper control of the sensitization and activation time as shown in Fig. 9d_3. It shows that the Pd nanoparticles have a diameter of about 15 nm. Without the

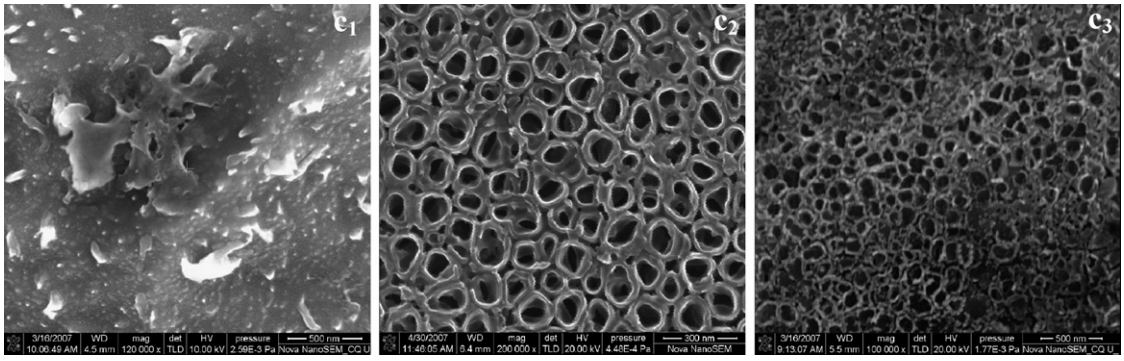

Fig. 7. FESEM images of TiO_2 films prepared at oxidation time of 10 min (c_1), 20 min (c_2) and 50 min (c_3).

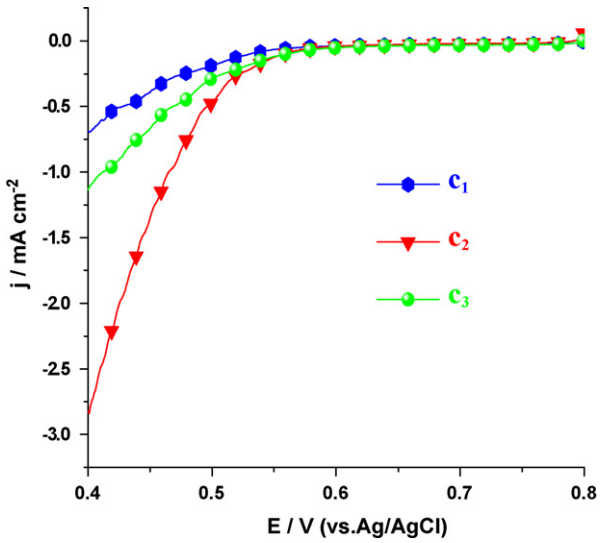

Fig. 8. LSV curves of ORR on Pd/TNTs/Ti at 1 mV s^{-1} where c_1, c_2 and c_3 denote the substrates TNTs/Ti as described in Fig. 7.

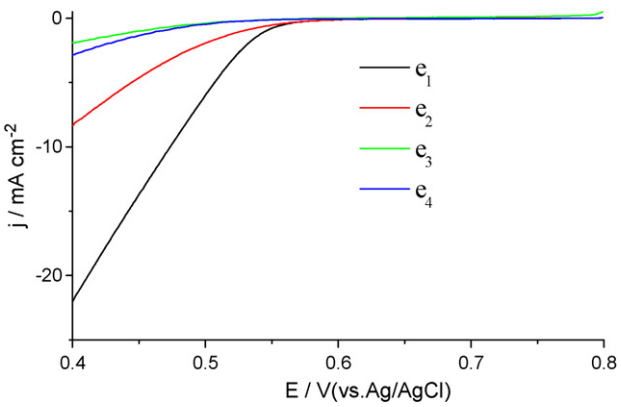

Fig. 10. Oxygen reduction on electrodes Pt/C (e_1), Pd/C (e_2), Pt/TNTs/Ti (e_3), and Pd/TNTs/Ti (e_4) in O_2 saturated 0.5 M H_2SO_4. The metal catalyst loadings was 0.27 mg cm^{-2}, 0.28 mg cm^{-2}, 0.30 mg cm^{-2} and 0.32 mg cm^{-2} for electrodes e_1, e_2, e_3 and e_4, respectively.

pre-sensitization and -activation on the surface of TiO_2/Ti, the surface state of TiO_2/Ti would be totally even. Thus, the following Pd electrodeposition would indiscriminately take place everywhere. This would lead to the formation of dense and poorly dispersed Pd deposits as shown in Fig. 9d_1. However, if the sensitization and activation last too long, too much Pd seeds would be generated. This again will lead to the formation of large and dense Pd deposits as shown in Fig. 9d_2. The highly dispersed nanopartilces are favorable and essential for the high performance and activity of the electrocatalysts.

3.5. Comparison between different catalysts

Fig. 10 presents the ORR on the electrodes of Pt/C made from Johnson-Matthey 40% Pt/C catalysts (e_1), Pd/C (e_2), Pt/TNTs/Ti (e_3), and Pd/TNTs/Ti (e_4) in O_2 saturated 0.5 M H_2SO_4. The metallic catalyst loadings were 0.27 mg cm^{-2}, 0.28 mg cm^{-2}, 0.30 mg cm^{-2} and 0.32 mg cm^{-2} for e_1, e_2, e_3 and e_4, respectively. As can be seen from Fig. 10, the current density for ORR on the Pd/TNTs/Ti is larger than

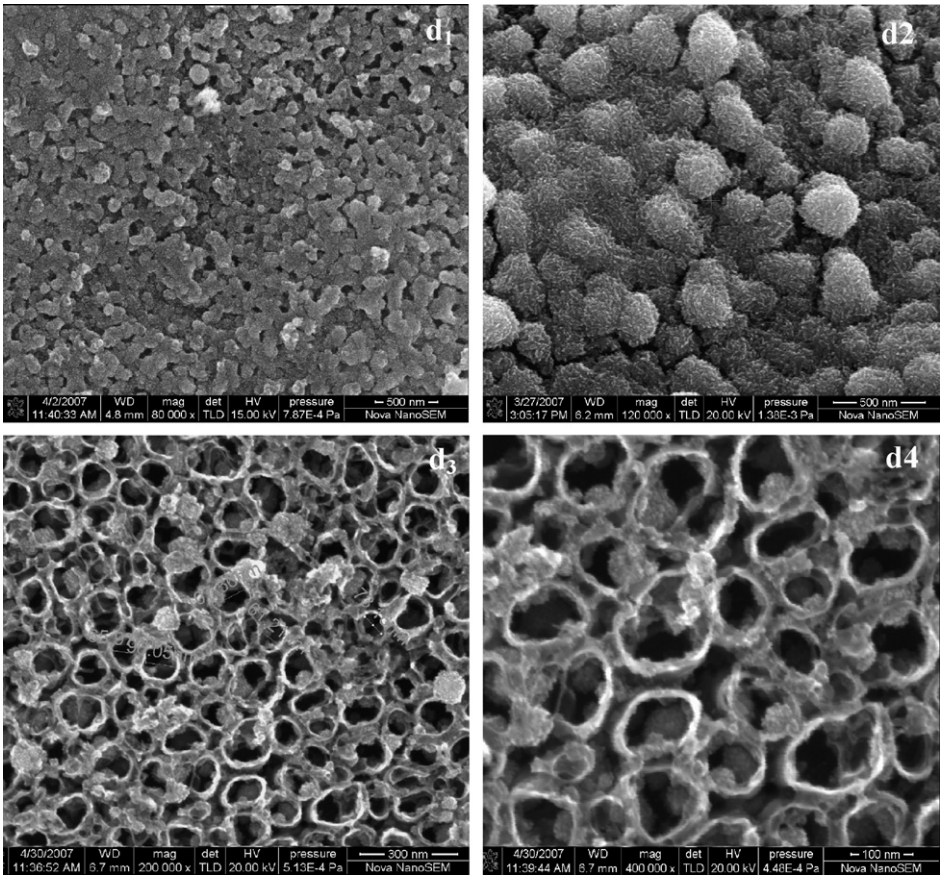

Fig. 9. SEM images of Pd deposited on TNTs/Ti supports treated at different sensitization and activation conditions. (d_1) No sensitization and activation, (d_2) with 10 min sensitization and 5 min activation, (d_3) with 5 min sensitization and 1 min activation and (d_4) amplified d_3.

that of the Pt/TNTs/Ti, but is smaller than that of Pd/C and Pt/C. The reason for the better activity of Pd/TNTs/Ti towards the ORR as compared to Pt/TNTs/Ti is that TiO_2 remarkably expands the space size of Pd/TiO_2 HOMO orbital and improves orbital overlap between Pd/TiO_2 HOMO and O_2 LUMO. In addition, the strong interaction between Pt and Ti in TiO_2 leads to a strong adsorption of the intermediate oxygen species from O_2 reduction on Pt/TiO_2, but the strong interaction between Pd and surface oxygen species in TiO_2 causes only a weak adsorption of the intermediate oxygen species from O_2 reduction on Pd/TiO_2 [11]. One reason for the low activity of Pd/TNTs/Ti as compared to that of Pt/C and Pd/C is that the Pd particle size dispersed on TNTs/Ti is much bigger than that of Pt dispersed on carbon powders. The Pd particle size is about 15 nm for Pd/TNTs/Ti as shown in Fig. 9d_3 but it is only 3 nm for Pt/C (Johnson-Matthey 40% Pt/C catalysts). The larger particle size means the less specific surface area of the catalyst particles and thus less active areas. In addition, the lower electric conductivity of TiO_2 relative to carbon also attributes to the small ORR current on Pd/TNTs/Ti. However, the Pt-free Pd/TNTs/Ti catalyst could be cheaper and TNTs/Ti as support is more stable in comparison with carbon at fuel cell operation conditions.

4. Conclusions

(1) Pulse anodic current oxidation method is superior to direct anodic current oxidation method for the production of highly ordered and uniform crystalline TiO_2 nanotubes in terms of time-saving and low operational temperatures.
(2) Chemical dissolution of TiO_2 in the HF-containing electrolyte plays a key role in forming TiO_2 nanotubes. There is a balance between the TiO_2 electrochemical formation and the TiO_2 chemical dissolution for obtaining highly ordered and uniform crystalline TiO_2 nanotubes which depends on the HF concentration.
(3) The formation of TiO_2 nanotubes begins with small pits that will act as the pore forming centers. With the increase in the time of pulse anodic current oxidation, the top surface of a fully developed nanotubes array starts to form. However, excess pulse anodic current oxidation will lead to the crack of the TNTs array due to the fact that the long TiO_2 nanotubes could not sustain the balance between the TiO_2 electrochemical formation and the TiO_2 chemical dissolution.
(4) It is very important to control the conditions of sensitization and activation on the surface of TNTs/Ti before the Pd electrodeposition in order to obtain the highly dispersed Pd deposits.

Acknowledgements

This work was financially supported by NSFC of China (20676156, 20806096), by the Chinese Ministry of Education (307021), Chongqing and Guangdong Sci&Tech Key Projects (CSTC2007AB6012, 2007Z1-D0051 and SKT [2007]17-11), and Chongqing University Postgraduates' Science and Innovation Fund (200701Y1A0260212).

References

[1] M. Lefevre, J.P. Dodelet, P. Bertrand, J. Phys. Chem. B 109 (2005) 16718.
[2] H. Meng, P.K. Shen, Electrochem. Commun. 8 (2006) 588.
[3] S. Yoshimoto, J. Inukai, A. Tada, T. Abe, T. Morimoto, A. Osuka, H. Furuta, K. Itaya, J. Phys. Chem. B 108 (2004) 1948.
[4] M. Lefevre, J.P. Dodelet, P. Bertrand, J. Phys. Chem. B 106 (2002) 8705.
[5] M.H. Shao, K. Sasaki, R.R. Adzic, J. Am. Chem. Soc. 128 (2006) 3526.
[6] J.L. Fernandez, V. Raghuveer, A. Manthiram, A.J. Bard, J. Am. Chem. Soc. 127 (2005) 13100.
[7] O. Savadogo, K. Lee, K. Oishi, S. Mitsushimas, N. Kamiya, K.I. Ota, Electrochem. Commun. 6 (2004) 105.
[8] P.K. Shen, C.W. Xu, Electrochem. Commun. 8 (2006) 184.
[9] V. Raghuveer, A. Manthiram, A.J. Bard, J. Phys. Chem. B 109 (2005) 22909.
[10] Z.W. Chen, M. Waje, Angew. Chem. Int. Ed. 46 (2007) 4061.
[11] L. Li, Z.D. Wei, Y. Zhang, M.Y. Xia, X.Q. Qi, Sci. China, Ser. B: Chem. 38 (2008) 769.
[12] J.E. Wijnhoven, W. Vos, Science 281 (1998) 802.
[13] J.N. Nian, H. Teng, J. Phys. Chem. B 110 (2006) 4193.
[14] P. Hoyer, Langmuir 12 (1996) 1411.
[15] C. Ruan, M. Paulose, O.K. Varghese, G.K. Mor, C.A. Grimes, J. Phys. Chem. B 109 (2005) 15754.
[16] M. Paulose, K. Shankar, S. Yoriya, H.E. Prakasam, O.K. Varghese, G.K. Mor, T.A. Latempa, A. Fitzgerald, C.A. Grimes, J. Phys. Chem. B 110 (2006) 16179.
[17] K. Shankar, G.K. Mor, A. Fitzgerald, C.A. Grimes, J. Phys. Chem. C 111 (2007) 21.
[18] Z.H. Zhang, Y. Yuan, Y.J. Fang, L.H. Liang, H.C. Ding, G.Y. Shi, L.T. Jin, J. Electroanal. Chem. 610 (2007) 179.
[19] S. Livraghi, A. Votta, M.C. Paganini, E. Giamello, Chem. Commun. 4 (2005) 498.
[20] G.K. Mor, K. Shankar, M. Paulose, O.K. Varghese, C.A. Grimes, Nano Lett. 6 (2006) 215.
[21] O.S. Alexeev, S.Y. Chin, M.H. Engelhard, L. Ortiz-Soto, M.D. Amiridis, J. Phys. Chem. B 109 (2005) 23430.